Vol. 16: 145–155, 2001 | CLIMATE RESEARCH Clim Res | Published January 18

The climate of Rome and its action on monument decay

D. Camuffo*, G. Sturaro

Consiglio Nazionale delle Ricerche - Istituto di Scienze dell'Atmosfera e del Clima, Corso Stati Uniti, 4, 35127 Padova, Italy

ABSTRACT: The 3-hourly standard meteorological data measured at Rome for the period 1951–1996 were analysed in order to gather information about the impact of climate on monument decay. The freezing-thawing and condensation-evaporation cycles in micropores were computed for each month. The occurrence of the freezing-thawing cycles was determined by means of a cross comparison between the temperature observations and the model calculations for the lowering of the freezing point due to the curvature effect of the ice surface into pores. The occurrence of the condensation-evaporation cycles was determined by means of a cross comparison between relative humidity observations and the lowering of the critical relative humidity for condensation into micropores due to the curvature of the water meniscus. The effect of sea spray on the lowering of the freezing point was calculated to evaluate the number of the freezing-thawing cycles on the surface or in the macropores contaminated by NaCl. Wind roses as well as the drizzle, rain, shower, hail, snow and fog roses were drawn in order to determine which vertical-surface orientations undergo wetting or washing out by meteoric water. Finally, the relevance of each of these meteorological variables was evaluated, evidencing the peculiarities of the region, which is influenced by both the Mediterranean climate and the cyclonic systems coming from the Atlantic Ocean.

KEY WORDS: Rome · Urban climate · Freezing-thawing cycles · Condensation-evaporation cycles · Precipitation roses · Monument decay

1. INTRODUCTION

The loss of cultural heritage is due to many environmental factors. The damaging effects of rare but extreme weather conditions (e.g. river flooding, gale winds or severe freezing) are obvious; but it is the almost invisible but constant damage caused by everyday weather conditions which has a cumulative and synergistic effect that in the long run is even more destructive (Koestler et al. 1994). Typical decay agents are daily temperature and humidity cycles, which determine mechanical stress and fatigue; alternation of condensation and evaporation; sea spray transport and deposition; salt dissolution and recrystallisation; mesomorphic transformation of minerals; and conditions favourable to biological life or chemical reactions. In addition, the combined effect of wind and precipitation determines the specific forms of wetting, washing out or the dangerous impact of hail on exposed surfaces. The aim of this paper is to analyse some meteorological variables in the context of urban Rome, in order to increase our understanding of monument weathering. This requires a non-traditional point of view which takes into account not only the bulk effect on the external surfaces of monuments, but also considers some processes occurring at the microscopic scale in the micropores (Camuffo et al. 1997, 1999a). Toward this end, it is more preferable to study the seasonal (and daily) cycle of the variables' frequency distribution than averages, i.e. the mean and the range of variability (the maximum and minimum values).

In this study, the 3-hourly data of the Italian Meteorological Service taken from 1951 to 1996 at the Ciampino Airport (13 km SE of the centre of Rome) were analysed, namely the freezing-thawing cycles,

*E-mail: camuffo@ictr.pd.cnr.it

the condensation-evaporation cycles, and the hydrometeor roses, i.e. the frequency distribution per 10° of wind associated with drizzle, rainfall, shower, hail, snow and fog. The methodology can be applied to other sites, but it is useful to understand the general characteristics of the place where monuments are located. Rome was chosen both because of the long-term exposure of its magnificent monuments and because of the interesting climatic characteristics. In fact Rome is located on the border of 2 different climatic regions and is thus influenced by both the European continental climate and the Mediterranean climate (Meteorological Office 1962, Mennella 1967, Reiter 1975, Cantù 1977); as a result, the rainfall in Rome (Eredia 1911, Colacino & Dell'Osso 1980, Colacino & Rovelli 1983, Camuffo 1993) is affected by both a typically Mediterranean character—with a rain season that lasts from November to April, reaching its maximum when the sea-air temperature difference is at its maximum—and by the penetration of the Atlantic perturbations in the mid seasons which affect the rest of Europe to the north of Rome.

2. TEMPERATURE DISTRIBUTION AND FREEZING-THAWING CYCLES

2.1. Temperature distribution

The frequency distribution of temperature values was analysed in 2 ways, using (1) the histogram of the population classes and (2) the percentile distribution. If the frequency distribution of a population X is symmetrical, the 50 percentile equals the mean value $<X>$. If the distribution is, in addition, Gaussian, then the 15 and 85 percentiles respectively equal nearly $<X> - \sigma$ and $<X> + \sigma$, where σ is the standard deviation.

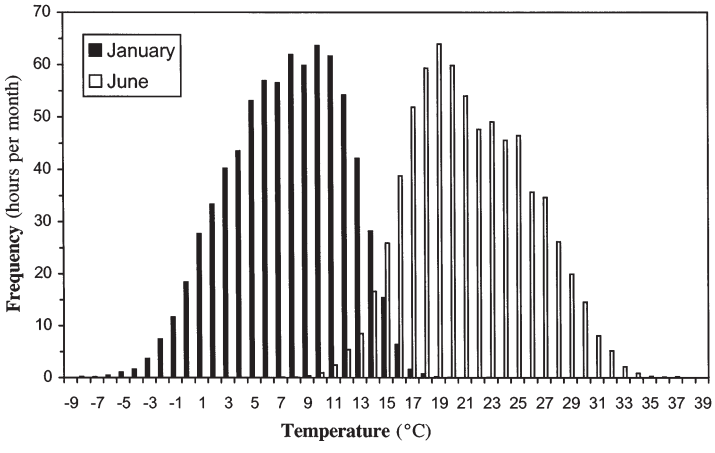

Fig. 1. Air temperature distribution in Rome in January and June

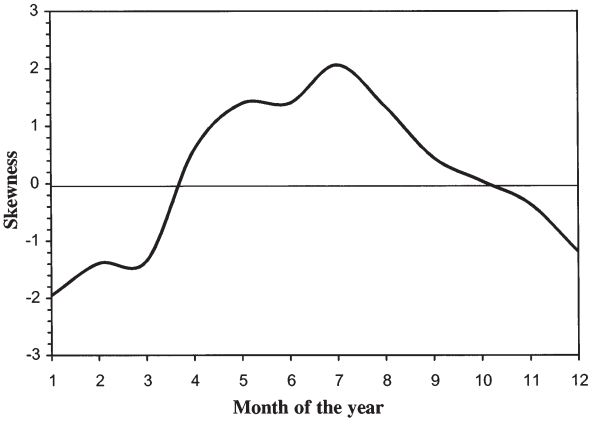

Fig. 2. Seasonal course of the skewness of the temperature distribution

The histograms show a monthly distribution which is almost symmetrical, Gaussian-like, but with a skewness generated by a higher frequency of cold episodes in winter and a higher frequency of warm episodes in summer (Fig. 1). The occurrence of the different episodes is well evidenced by the Pearson first coefficient of skewness, defined as

$$S_k = 3(<X> - m)/\sigma$$

where m is the mode. The Pearson coefficient oscillates during the year, ranging from –2 in January to +2 in July (Fig. 2). The skewness is useful to highlight significant departures from the average meteorological conditions. In winter, the negative skewness shows that extreme events of cold weather are more probable than equivalent warm-weather departures. Therefore, even in a mild winter, the risk of freezing is always present. In the 2 mid seasons, the skewness is nearly zero, and cold or hot anomalies are equally probable. In summer, the skewness is positive, and the probability of it being extremely hot (and de-hydrating a monument, or causing structural stress) is higher than that of mild weather occurring. During extremely hot episodes, on sunny days the bronze statue of Marcus Aurelius (now kept indoors) was some 15°C hotter than the air, while during the night its temperature was equal to the air temperature, as is usually the case for this kind of monument (Camuffo & Vincenzi 1985). Thus the daily temperature cycle of the statue was some 25°C. On these hot days the expansion of the bronze exceeded the expansion of the marble basement by approximately 0.5 mm, and this difference was transformed into a tension exerted on the 3 horse hooves connected to the white marble basement.

The large thermal inertia of massive buildings protects them from freezing during sudden epi-

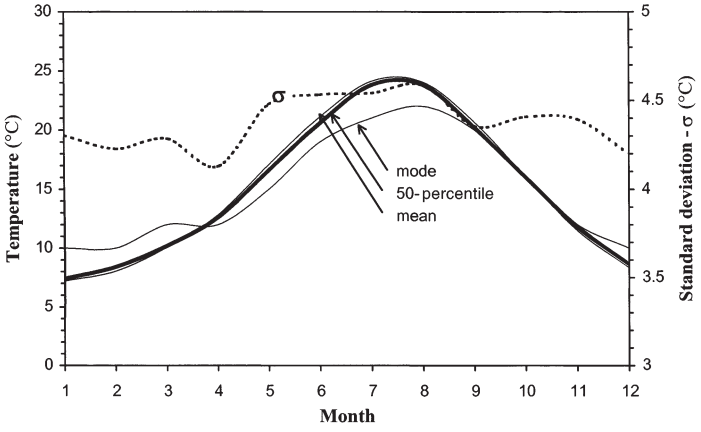

Fig. 3. Seasonal course of mode, mean, 50 percentile and standard deviation (σ) of the air temperature

sodes of below-zero temperatures; in contrast, decorations and architectural details with a small inertia follow the air temperature changes quite closely and for this reason are exposed to greater stress. However, a negative effect of a large thermal inertia occurs in the winter when the sirocco wind blows warm and humid air which immediately condenses on the cold massive structures, e.g. the Colosseum, forming a thin layer of water.

Percentile distributions were calculated for the monthly values of air temperature. Distributions are not completely symmetrical and Gaussian-like; the mean is very close to the 50 percentile (Fig. 3), and the plots of these 2 variables are practically indistinguishable. However the most typical meteorological situation, shown by the mode, is different. Mean temperature values range from 7.2°C in January to 24.1°C in July. The variability of temperature in the course of the year is given by the standard deviation which is a little higher in summer, although it remains ~4.5°C (Fig. 3).

For each month, percentile distributions were also calculated for 3-hourly values of air temperature, aggregating the values according to the hour of measurement. From the analysis, the daily variations are well defined, month by month. In January (Fig. 4) the 50 percentile reaches its daily minimum value at 4.6°C and its maximum at 11.2°C, and in August at 19.4°C and 29.4°C respectively; the thermal span between night and day ranges from 6°C in December to 10°C in July. As far as thermal expansions and contractions are concerned, the summer is thus the period of the year when the mechanical stress is higher, enhanced by the heating from direct solar radiation in those parts of the monuments exposed to sunlight. The complete percentile distribution offers important additional information, e.g. the occurrence of rare and extreme events, and makes possible further analyses of the temperature cycles (see next section).

2.2. Freezing-thawing cycles

Freezing damage occurs especially in the climatic regions where the temperature oscillates around zero; this situation is reached in Rome only occasionally as the mode in January is +10°C. In the case of freezing, ice crystals start forming in the large pores at zero temperature; they eventually grow, sucking supercooled liquid water from finer pores, which behave like water reservoirs. The most severe damage occurs in materials having medium to large pores, where ice crystals form and grow. Ice crystals may also form in the finest pores, where the transition of state occurs at very low subzero temperatures, when the temperature drops below a critical point determined by the radius of curvature of the supercooled water meniscus (Everett 1961, Fagerlund 1973, Clifford 1981, Iribarne & Godson 1986, Camuffo 1998). If the finest pores are connected to macropores through capillaries filled with water, they have a good probability of remaining empty after transferring their water to the ice crystals growing in macropores. However, if the connection capillaries are empty, the micropores have a high probability of being filled with water from early condensation, as given by the Kelvin effect; in this case the frost damage occurs only at very low temperatures. The lowering of the freezing point ΔT_f by the curvature effect of the water meniscus in micropores having radius r is given by the equation

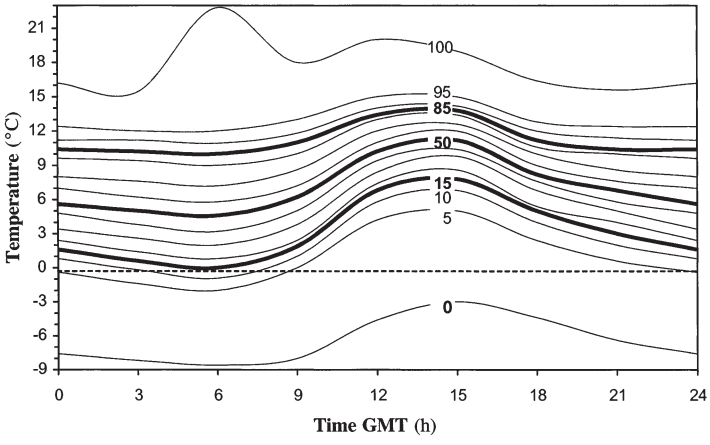

Fig. 4. Daily percentile distribution of air temperature in January. Note that local time (LT) is GMT + 1. Dotted line: 0°C

$$\Delta T_f = T_f \frac{2\sigma_{sl}}{r \rho_s L_f}$$

where σ_{sl} is the surface tension at the solid-liquid interface, ρ_s the ice density and L_f the latent heat of fusion. At 0°C the liquid water freezes on the smooth, uncontaminated surfaces. Calculation shows that at a temperature of –0.97°C freezing occurs in all the pores with a radius larger than 0.03 µm, at –2.91°C in pores larger than 0.01 µm, at –5.71°C in pores larger than 0.005 µm, and at –9.4°C in pores larger than 0.003 µm. Therefore, the frost action depends upon 3 factors: (1) the behaviour of water at subfreezing temperatures and its migration inside the rock; (2) the intensity, rate and duration of freezing; and (3) the properties of the rock, including pore size distribution, which controls water saturation and lowering of the freezing point (Lunardini 1991, Gauri & Bandyopadhyay 1999).

In Rome the winter is mild and the surface of monuments is the part most exposed to the risk of frost damage. Brick buildings, sandstone walls and decorations, characterised by large pores, are most at risk. The white Carrara marble of the most famous works of art, such as the Trajan Column or the Ara Pacis, is characterised by very fine micropores where ice crystals can only form in exceptional conditions. The absence of frost damage has been confirmed by the careful analysis of these monuments.

The calculation of the number of freezing-thawing cycles in Rome was made in the following way: For the months with sub-zero temperature values in the plots of the kind shown in Fig. 4, horizontal lines corresponding to the freezing points were drawn. The lines intercept some of the isopercentile curves. The intercepts represent a change of state undergone by the water trapped in the stone micropores in thermal equilibrium with the atmosphere. Looking at only 1 line, the maximum and minimum percentile values of the isopercentile curves intercepting that line were determined. The difference between the maximum and minimum percentile value is the percentage of the days during which freezing-thawing cycles occurred during the month. The method can be more clearly understood by looking, for example, at the zero temperature line drawn in Fig. 4 for January. The 15 percentile curve is the greatest percentile curve intersecting the line, while the smallest is the 2 percentile curve (not drawn); thus, in 2% of the days in January the temperature is always below zero, in 13% of the days a cycle around zero occurs and for the rest (85% of the days) freezing never occurs. Calculations were then made for every month and the critical subzero temperatures corresponding to the freezing point of the above indicated micropore sizes.

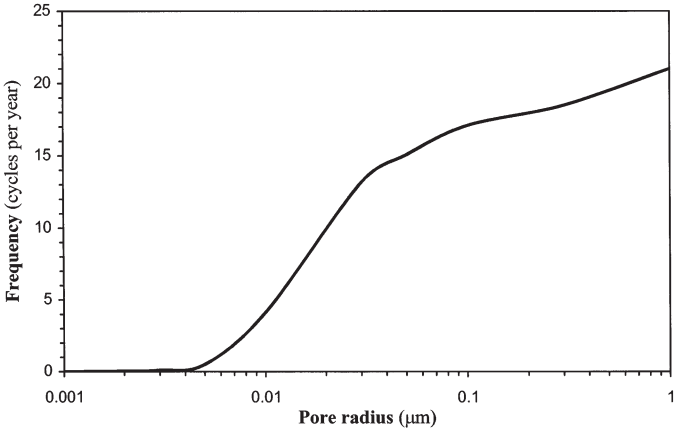

Fig. 5. Freezing-thawing cycles per year versus pore radius, calculated using the observed temperature distribution and the Kelvin law

Table 1. Average time (h) per month during which air temperature T_{air} goes below a certain freezing value

T_{air} (°C)	Month of the year 1	2	3	4–10	11	12	Yearly total
–8	0.20	0	0	0	0	0	0.20
–7	0.13	0	0	0	0	0	0.13
–6	0.46	0.13	0	0	0	0	0.59
–5	1.05	0.13	0.26	0	0.07	0	1.51
–4	1.65	0.66	0.53	0	0.07	0.33	3.24
–3	3.69	1.85	1.05	0	0	0.92	7.51
–2	7.45	4.55	2.31	0	0.20	2.44	16.95
–1	11.67	7.91	3.43	0	1.25	5.21	29.47
0	18.40	12.59	4.95	0	1.71	10.68	48.33
Total below 0°C	45.70	29.82	15.53	0	14.30	31.58	136.93

In Rome, the freezing-thawing cycles (Fig. 5) are fortunately not very frequent, i.e. 21 yr^{-1}, and their frequency decreases when smaller pores are considered. For pores with a radius of 0.01 µm the frequency is reduced to some 4 cycles yr^{-1}, and for 0.005 µm pores to 1 cycle every 2 yr; for pores with a radius smaller than 0.003 µm such cycles are rare. The number of cycles was also counted by looking directly at the time series; practically the same results were obtained. By this method other information can be gathered, for example, the length of cycles, i.e. the persistence of freezing, which can be important when considering the interior of monuments. In fact, if air temperature drops for a short time below zero, the cold cannot penetrate deeply into monuments and form ice crystals. Only in 2 cases did freezing last more than 24 h, and only in 1 case more than 36 h. From these figures and from the statistics of the time during which temperature is equal or below 0°C (Table 1), it is evident that

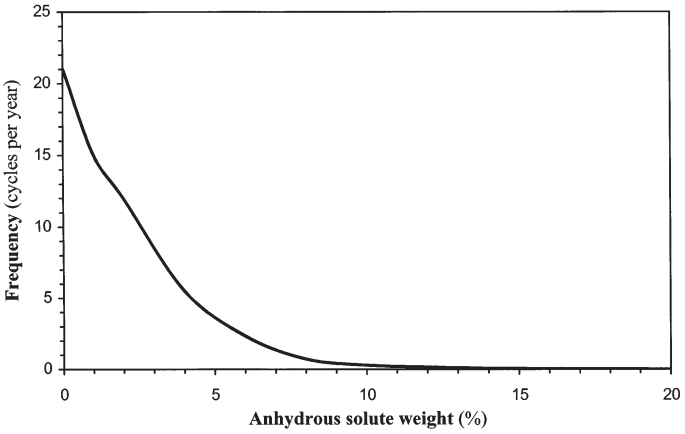

Fig. 6. Freezing-thawing cycles per year due to NaCl contamination expressed as percentage of anhydrous solute weight

freezing in Rome is not a major concern; this is also true for the past centuries, at least for 2 millennia (Camuffo 1993).

2.3. Sea-spray and freezing-thawing cycles

So far it has been assumed that the pores were uncontaminated, and the Kelvin theory for pure ice has been applied. In the presence of soluble salts the freezing frequency is reduced and lower temperatures, below zero, are needed. Rome is located 25 km from the sea and thus marine aerosols are deposited on monuments. In normal conditions, marine aerosols mainly originate from bubbles in whitecaps, i.e. from the disintegration of the film that forms the cap of the bubble, or from the central jet that forms when the cavity of the bubble collapses; the jet drops seem to be the main source of the so-called giant salt nuclei in the atmosphere (Kraus & Businger 1994, Brimblecombe 1996). During storms, the gale wind is much more effective in breaking waves, transferring from the sea to the atmosphere large amounts of water, which is immediately transformed into spray.

It is well known that NaCl contamination is detrimental to conservation as it is deliquescent at 75% relative humidity and over this humidity level the contaminated surfaces become wet. As a consequence, the time of wetness is heavily increased with many negative consequences, e.g. speeding up the chemical reactions and favouring (micro)biological life. Direct salt decay is generated by crystallisation, hydration, differential thermal expansion and osmosis (Arnold & Zhender 1990, Winkler 1994, Zezza 1996, Pombo Fernandez et al. 1999). Sea salt contamination has many negative consequences on stone weathering, and the combined action of salt and other forms of physical weathering has dramatic consequences. However, what about the NaCl effect on freezing-thawing cycles? The lowering of the freezing point is given by

$$\Delta T_f = K_f m$$

where K_f = 1.86 K mol^{-1} is a constant and m is the solute molality (Weast 1985, Adamson 1986). The number of freezing-thawing cycles (Fig. 6) decreases from 21 yr^{-1} for extremely low contamination, becomes 3 cycles yr^{-1} at some 5% solution (anhydrous solute weight) and vanishes at 10% solution. Although the influence of sea salt on the reduction of freezing-thawing cycles is positive, the other negative impacts are clearly dominant, and NaCl contamination should be considered a very detrimental factor.

3. RELATIVE HUMIDITY DISTRIBUTION AND CONDENSATION-EVAPORATION CYCLES

The histograms of the relative humidity show a distribution substantially different from that of air temperature. In winter, the frequency increases with the humidity level, showing an exponential distribution up to 90–95% (Fig. 7). In the other months smaller values become more frequent and the distribution is broader: in July values ranging from 45 to 90% have approximately the same frequency. The skewness S_k lies between –4 and –2, with a higher value of –1 in July; the variance ranges from $\sigma \approx 14\%$ in winter to ~18% during summer (Fig. 8). The asymmetry of the distribution leads to different values for the average, 50 percentile and mode (Fig. 8). In this case, a

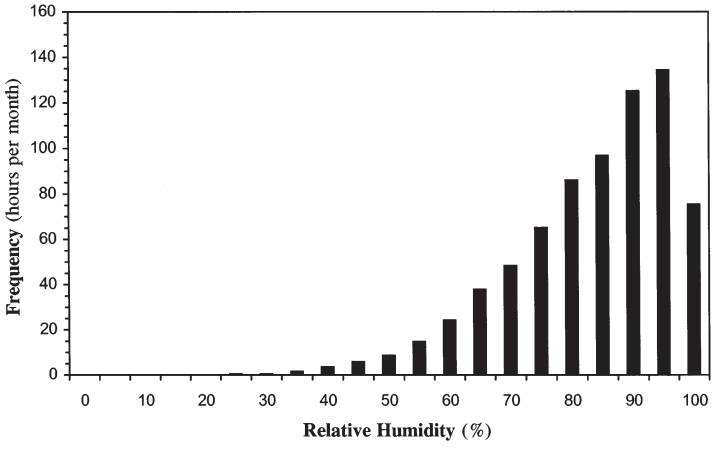

Fig. 7. Relative humidity distribution in December

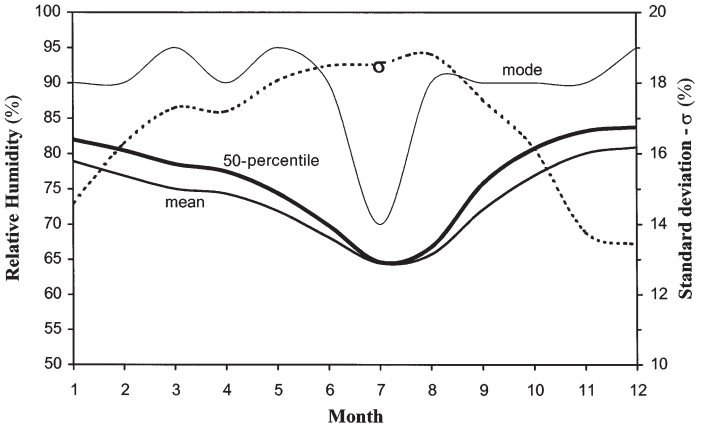

Fig. 8. Seasonal course of mode, mean, 50 percentile and standard deviation (σ) of the relative humidity

description of this parameter based on averages is poorly representative of the typical climatic features, which are better represented by the frequency distribution.

Again, for each month, percentile distributions were also calculated for 3-hourly values, aggregating relative humidity values according to the time of observation. These percentile distributions (Fig. 9) show the daily variation of the parameter. In December, the 50 percentile reaches its daily minimum value of 69% in the hottest hours and its maximum of 89% during the night; in July it ranges from 44 to 82%. The distribution is useful to measure the frequency of the condensation-evaporation cycles in the micropores. This phenomenon is governed by the Kelvin law, which determines for each spherical pore with radius r a critical value of relative humidity RH that triggers condensation

$$RH(r) = 100\exp\left(\frac{2\sigma_w V_m}{rRT}\right)$$

where σ_w is the surface tension of water, V_m the molar volume of water, R the gas constant and T the temperature of the thermodynamic system in equilibrium (Mason 1971, Camuffo 1984a, 1998). This equation, specific to the more common spherical pores, can be adapted for other pore geometries by replacing $2/r$ with dS/dV (where S is the water meniscus surface and V the water volume). For example, in granite cylindrical menisci are formed and $dS/dV = 1/r$.

When the ambient relative humidity is lower than the critical value for a pore size, the pore is empty; when it is higher, the pore is full of water. When the ambient relative humidity crosses the critical value a change of state occurs. The daily course of relative humidity percentile distributions in August (1956–1995) is shown in Fig. 9. The condensation-evaporation cycles were counted for certain relative humidity critical values: namely 58.7, 70.1, 80.8, 89.9, 96.5, and 98.9%, which are the critical values for spherical pores with radius 0.002, 0.003, 0.005, 0.01, 0.03 and 0.1 µm respectively. Bigger pores should be full of water at 100% relative humidity, because the small departure due to the Kelvin effect falls within with the experimental errors in measuring relative humidity. The data analysis (Fig. 10) was undertaken with the same method used to calculate freezing-thawing cycles (see above). Fig. 10 shows the number of condensation-evaporation cycles for each pore size, as well as the number of days per year in which pores remain filled with water or empty, as a function of their size. The highest frequency of condensation-evaporation cycles is experienced by micropores with a radius in the 0.004 to 0.005 µm range, with more than 300 cycles yr^{-1}. These are the pores at higher risk as far as dissolution, recrystallisation and desegregation are concerned. The same calculation applied to data taken at the Basilica of Santa Maria Maggiore, in the city centre, showed the same frequency; however, the maximum was slightly displaced, to between 0.002 and 0.003 µm. Inside the Basilica the frequency was nearly halved, and the distribution shifted to a maximum at 0.002 µm (Camuffo et al. 1999b). Of course, this calculation was made with regard only to the pure Kelvin effect from the meniscus curvature on pure water. The real case is complicated by contamination with other soluble salts, which displace the equilibrium towards condensation at lower values of relative humidity. This is equivalent to saying that in porous material the condensation is displaced towards pores having a greater size. In fact, the susceptibility of porous materials to salt crystallisation

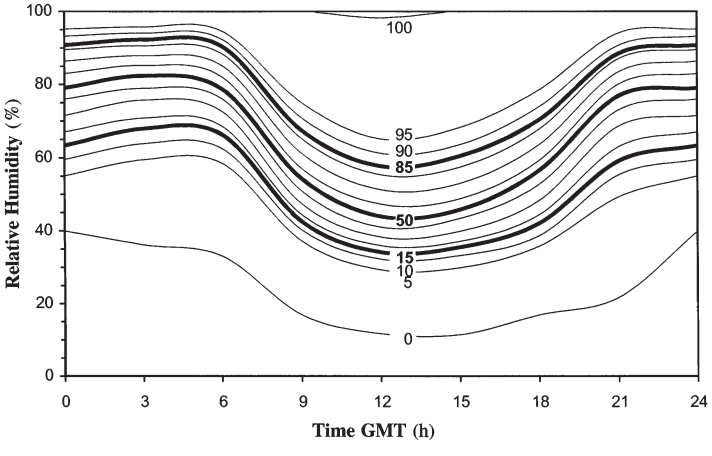

Fig. 9. Daily percentile distribution of relative humidity in July

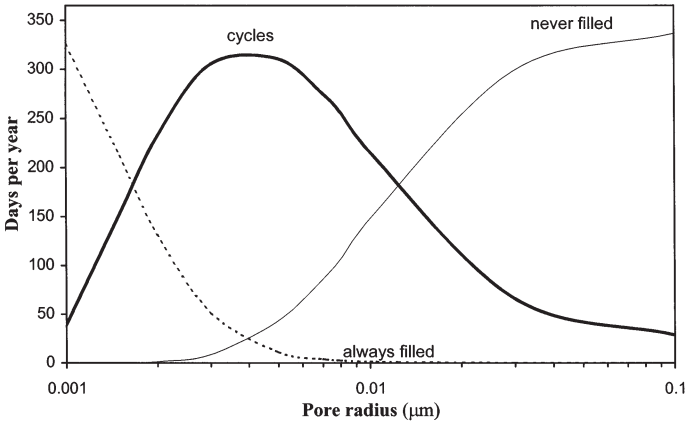

Fig. 10. Yearly number of days on which condensation-evaporation cycles occur and on which pores always remain or are never filled with water versus pore radius

damage appears to be related to the pore size distribution and pore volume of the material (Ginell 1994).

The damage due to the Kelvin effect and the condensation-evaporation of water inside the micropores is manifold. Water supplied in condensation causes the dissolution of the material matrix, and the cycles determine the migration of dissolved salts and their recrystallisation in other parts. Water reduces the mechanical resistance of some materials, e.g. rock and mortars. The presence of water of course favours chemical reactions, and decay due to air pollution or particle deposition is enhanced.

From Fig. 10 it is clear that, while larger pores are only slightly affected by condensation, the finest pores tend to always remain filled with water and they constitute a reservoir of water for biological life. For this reason the study of the occurrence of condensation in micropores is fundamental to an understanding of biocontamination and biodecay of outdoor monuments. Even in dry environments the presence of water in micropores makes colonisation by bacteria, algae and other micro-organisms possible. In the case of the Trajan Column, pitting by lichens is evident in some positions where the bas-relief geometry is horizontal and is able to collect water droplets either from direct condensation as dew or from rain (Camuffo 1993). Lichens were able to grow because of this form of water-droplet collection; however, they do not live on the Column anymore, having been killed by SO_2, which is very toxic for lichens. Rotifers and algae can live in the micropores of the subsurface layer due to the water contained there (Del Monte & Sabbioni 1986, Del Monte 1991).

In monuments the effective time of wetness is in practice determined by 3 key factors: the wetting due to rainfall, the surface condensation at dew point temperature (which may be lowered by the presence of deliquescent salts) and the condensation in micropores. In these wider terms the corrosion of the bronze statue of Marcus Aurelius has been studied with success (Laurenzi Tabasso & Marabelli 1992).

4. THE HYDROMETEOR ROSES

The wind rose has a seasonal character. In the cold season, approximately from October to March, the main winds are the 'Borea' from the NE (catabatic local wind, channeled in by the Apennines over the Tiber Valley) and the 'Sirocco' from SSE (warm and humid wind coming from North Africa). During the hot season, the dominant winds generally stop and a breeze occurs. The wind rose changes: the NE wind is still present in the direction of the land (night) breeze, but the wind mainly blows from the whole third sector, which also contains the direction of the sea (day) breeze, as is evident from the summer roses at 15:00 h GMT, corresponding to 16:00 h local time (Fig. 11). This is the wind that brings sea-spray to the city. A direct correlation between the wind direction and each hydrometeor showed the following results:

Drizzle is associated with winds from the NE and from the sectors between the S and SSE (Fig. 12). The fine drizzle droplets (i.e. from 0.2 to 0.5 mm) are air-

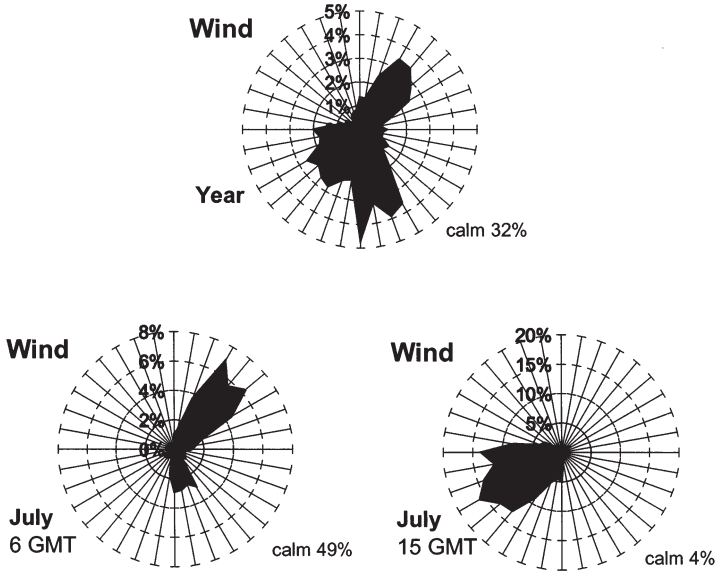

Fig. 11. Wind roses: yearly total distribution of the wind and July distribution showing the land breeze at 06:00 h GMT = 07:00 h LT (local time) and the sea breeze at 15:00 h GMT = 16:00 h LT

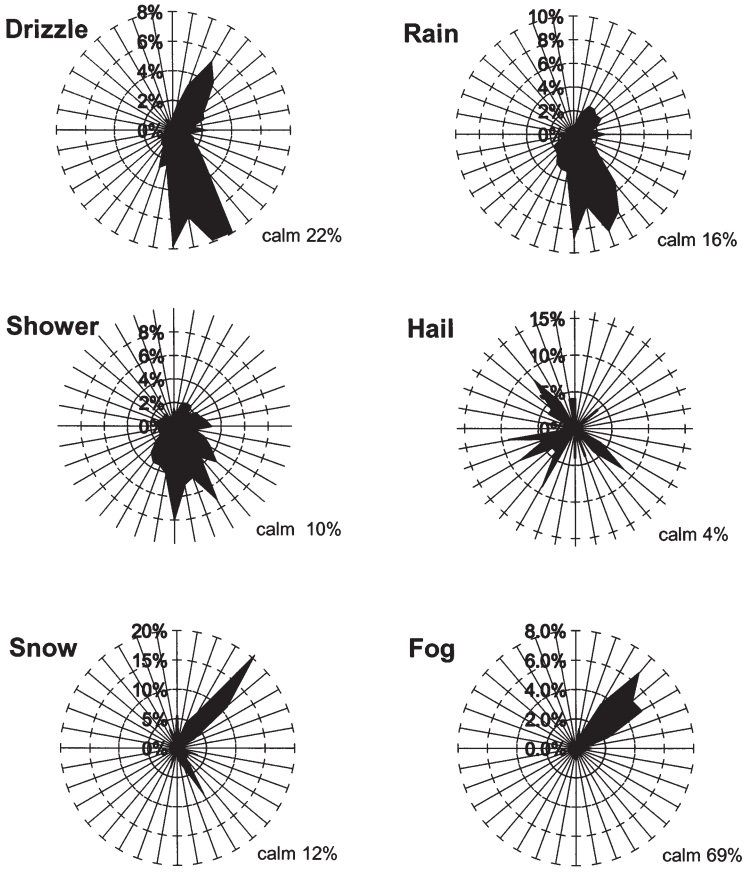

Fig. 12. Roses of drizzle, rain, showers, hail, snow and fog

borne and follow the wind streamlines rather well. As a consequence, they impact the surfaces facing the wind only in small numbers; however they impact the surfaces parallel to the wind stream (where turbulence develops) much more—wetting them.

The *rain* distribution is similar to that of drizzle, but is mainly associated with a southern wind direction (Fig. 12). As a consequence, during rainfall airborne droplets (whose size lies between 0.5 to 6 mm diameter) because of their inertia force splash on surfaces exposed mainly to the sector between the S and SSE, washing them out. Looking at the buildings of Rome, e.g. the Colosseum (Camuffo 1998), the walls of the upper floors are more washed out due to the greater force of the wind. At lower levels drops fall more vertically, given the lower wind speed, or are intercepted by the nearby buildings; this fact, together with the greater concentration of particles emitted by traffic, contributes to make the lower floors darker.

Intense precipitation and large droplets during *showers* splash with a slightly greater variability, although winds from the S sector are dominant (Fig. 12).

Hail is very rare, and the directions from which it comes from are scattered (Fig. 12).

Snow (Fig. 12) presents a different pattern; it is associated with the local NE wind.

Fog forms in the Tiber Valley and is transported to Rome by local circulation channelled by the valley itself (NE); however, a slow wind speed is often associated with the fog, as 69% of the fog episodes occur during calm conditions (Fig. 12). The very fine droplets (i.e. smaller than 0.2 mm) have a very small inertia and closely follow the streamlines. As a consequence the surfaces the droplets have the highest probability of impacting are not those facing the wind, but those parallel to it, where turbulence develops. However, the number of droplets which will impact a surface at a low wind speed is very small, and the surface wetting occurs via another mechanism. During fog, the air temperature equals the dew point or is slightly above it (e.g. relative humidity in the range 95 to 100%). When the surface temperature of monuments is below the air temperature, it is also below the dew point, and thus condensation occurs on the surface. The liquid film of water and the droplets found on the surface are chiefly the result of direct condensation, not of droplet impact. In the former case, wetting depends upon the surface temperature and is irrespective of airspeed direction.

The seasonal distribution of the above precipitation types is shown in Fig. 13. Drizzle appears only in the winter (when it is present 2% of the time) and the mid seasons; from May to October it occurs less than 0.5% of the time. The rain frequency has a maximum in November (7.5% of the time) and continues for the whole cold season. The minimum is in July, slightly less than 0.5%. Showers are relatively short and infrequent, so that this intense precipitation shows a maximum of occurrence of 1% of the time in September and October. Similarly, hail is rare and short-lived; it has two maxima, one in April when it occurs for 0.04% of the time and another one in December when it falls 0.08% of the time. Snow flakes fall in the period from October to March; however, snowfall is rare, as the maximum frequency is some 0.3% of the total time of February. Fog too is a typical winter phenomenon, reaching maximum frequency in December, but it lasts only some 1.3% of the whole time during this month. Rain is then the main hydrometeor falling in the Rome area and its seasonal course is of mixed type. The Mediterranean character is evident, with precipitation occurring in the cold season, when instability develops

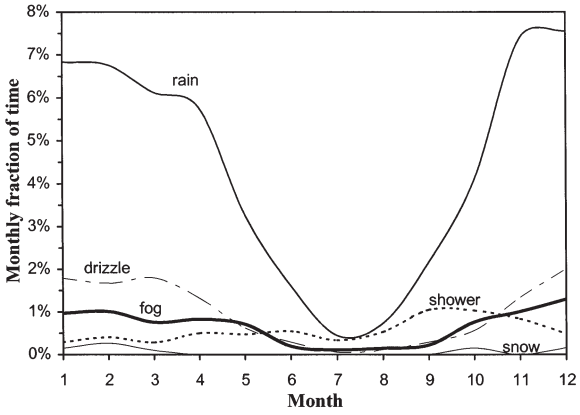

Fig. 13. Seasonal distributions of drizzle, rain, showers, snow and fog, expressed as a percentage of time of each month

because the sea water is warmer than the air. The maximum rain frequency occurs in November and not when the sea-air temperature difference is at its maximum, showing the influence of the autumnal penetration of Atlantic perturbations into the Mediterranean, when the Azores anticyclone is not yet developed. Another consequence of the latter influence is that, looking at the amount of precipitated water, the maximum is found earlier, in October, followed by November and December (Colacino & Purini 1986, Mangianti & Beltrano 1995). The spring penetration of the Atlantic perturbations is connected with the rain frequency in April, which is only slightly less than that in March.

In addition to the precipitation, stone wetting occurs when vapour condenses on surfaces with a temperature below the dew point. On the walls of the historical buildings and on mainly vertical monuments, dew rarely forms as a result of the typical infrared loss of heat on clear nights. In fact, the vertical surfaces mainly irradiate horizontally, exchanging heat with the surrounding buildings and air; their heat loss is much less than that of the soil, which irradiates against the clear sky. Heavy condensation, characterised by the formation of large surface droplets, occurs when the warm, humid sirocco (with a relatively high dew point) blows in the cold season. The monuments, with their large thermal inertia, remain cold, below the dew point of the tropical air masses transported by the sirocco, and condensation occurs immediately.

Monuments such as the Trajan Column or the Aurelian Column that are completely exposed to atmospheric agents are very good examples of how the characteristics of stone decay vary with degree of exposure according to the hydrometeor roses. It was noticed that the sector between the SSE and S is where dissolution of stone is most evident, and this fact is explained by looking at the rain and shower roses (Camuffo 1993, Camuffo & Bernardi 1993). In the southern sector the marble surface recession has been evaluated to be 2 mm, making reference to the insoluble oxalate patina which still preserves signs of the original carving. Therefore, marble dissolution has proceeded at a rate of 1 µm yr^{-1}. The sides of stones exposed to windborne droplets are characterised by the presence of algae, mosses or plants, especially in the case of porous bricks or stones, where the amount of water collected after each period of precipitation is high (Caneva et al. 1992). On bronze monuments, the side exposed to windborne rainfall is altered and enriched in SnO_2, as was recognised by studying the Marcus Aurelius statue (Laurenzi Tabasso & Marabelli 1992).

Black crusts, mainly composed of gypsum with embedded soot and fly ash, form on the parts of monuments where rainwater cannot wash away the particles of pollutants deposited there. In contrast, the parts of marble or limestone monuments exposed to rainwater and washing out are white, and clean; the surfaces retreat due to dissolution and loss of material, and they are covered with small crystals of precipitated calcite that form when the rainwater, with dissolved calcium carbonate, evaporates (Camuffo et al. 1982, 1983, Camuffo 1984b, 1990, 1993, 1998, Laurenzi-Tabasso & Marabelli 1992, Camuffo & Bernardi 1993, Lorusso et al. 1995).

5. CONCLUSIONS

In Rome, 2000 yr old buildings and monuments are exposed to weather conditions which have a mixed character of the Central Eastern Mediterranean basin and Continental Europe, with precipitation in the cold and mid seasons and a dry summer. The frequency of precipitation evidences the climatic character of Rome: precipitation is more frequent during the autumn and winter period, i.e. when the thermal difference between the air and the warmer Mediterranean waters causes instability and frequent rainfalls. The influence of the Atlantic per-turbations shifts the maximum rainfall frequency to November, i.e. earlier than the period of maximum thermal difference between air and sea. Frigid winters are rare with the temperate sea influence, and only 21 cases of freezing-thawing cycles occur per year on average. In the micropore interior, this frequency is further reduced by the influence of the curvature of the water meniscus according to the Kelvin law. The presence of a curved meniscus lowers the freezing point below 0°C, e.g. pores with radius of 0.01 µm undergo only 4 cycles yr^{-1}, and for the finest pores freezing is negligible. In addition, as the surfaces of buildings and monuments are contaminated by

marine aerosols transported to the mainland by the sea breeze, the freezing frequency is further lowered. This means that in Rome, although temperature cycles around zero occur with a certain frequency in the free air, freezing-thawing cycles only exceptionally affect monuments and do not constitute a serious risk of decay. More detrimental is the role played by sea spray and air pollution with dissolution-recrystallisation cycles.

The typical dew with the nocturnal infrared loss is of minor relevance for historical buildings and monuments, as the liquid water formed by dew on a vertical surface on a clear night is of the order of a few tenths of a millimeter (Camuffo 1998). Much more relevant is the arrival of warm, humid air transported by the sirocco wind in the cold season which forms abundant condensation on massive stone monuments whose temperature remains below the dew point. Although Rome is not a humid city, with the Kelvin effect the condensation-evaporation cycles are much more frequent inside micropores than in the free air. They constitute an important cause of stone deterioration in Rome. The critical factor is that almost every day the 80% relative humidity level is crossed, with lower values during the day and higher values during the night. The consequence is that more than 300 cycles are experienced in micropores with a radius of 0.004 to 0.005 µm; thus dissolution-crystallisation cycles or water supply for biological life occur nearly every day. Thus, endolithic algae and rotifers live in the rock pores of the monuments, as is the case for the Trajan Column and other marble monuments.

The hydrometeor roses show which monument surface is more often wetted or washed during precipitation events: During rain and showers, the wind generally blows from the SSE and secondarily from the NE, and the surfaces exposed to these directions are wetted. Drizzle is transported by the same winds, but as the droplets are very small they follow the air streamline and impact the surfaces parallel to the wind, where the turbulence is greater, much more. Snow comes from inland with a NE direction. Fog is formed in the Tiber Valley and is transported to Rome when the wind blows in that direction, i.e. from the NE; the very small droplets wet the surfaces facing to the NW and SE, parallel to the wind. The most visible effects on monuments are: (1) stone dissolution and surface retreat in the parts of marble or limestone monuments exposed to run-off; (2) formation of black crusts which include fly ash and soot deposited in the parts not reached by wash out; (3) growth of algae, mosses and also plants in the parts of porous materials exposed to rainwater, where large pores may keep a reservoir of water for a long time; and (4) leaching and alteration of the surface patina of bronze monuments.

Acknowledgements. This work was supported by the European Commission, Programme Environment, contract ENV4-CT95-0092 ARCHEO, aimed at identifying the past and natural weathering of monuments in order to distinguish it from the present day cumulative effect and at arriving at a sound predictive scenario about the cultural heritage. The meteorological data were gathered by the Meteorological Service of the Italian Air Force.

LITERATURE CITED

Adamson AW (1986) A textbook of physical chemistry. Academic Press, San Diego

Arnold A, Zhender K (1990) Salt weathering on monuments. In: Zezza F (ed) The conservation of monuments in the Mediterranean Basin. Grafo, Bari, p 31–58

Brimblecombe P (1996) Air composition and chemistry. Cambridge University Press, Cambridge

Camuffo D (1984a) Condensation-evaporation cycles in pore and capillary systems according to the Kelvin model. Water Air Soil Pollut 21:151–159

Camuffo D (1984b) The influence of run-off in weathering of monuments. Atmos Environ 18:2273–2275

Camuffo D (1990) Acidic precipitation research in Italy. In: Bresser AHM, Salomons W (eds) Acidic precipitation, Vol 5. Advances in environmental science. Springer Verlag, New York, p 229–265

Camuffo D (1993) Reconstructing the climate and the air pollution of Rome during the life of the Trajan Column. Sci Tot Environ 128:205–226

Camuffo D (1998) Microclimate for cultural heritage. Elsevier, Amsterdam

Camuffo D, Bernardi A (1993) Microclimatic factors affecting the Trajan Column. Sci Tot Environ 128:227–255

Camuffo D, Vincenzi S (1985) Computing the energy balance of a statue of bronze: the San Marco's Horses as a case study. Sci Tot Environ 44:147–158

Camuffo D, Del Monte M, Sabbioni C, Vittori O (1982) Wetting, deterioration and visual features of stone surfaces in an urban area. Atmos Environ 16:2253–2259

Camuffo D, Del Monte M, Sabbioni C (1983) Origin and growth mechanisms of the sulphated crusts on urban limestone. Water Air Soil Pollut 18:351–359

Camuffo D, Sturaro G, Valentino A (1997) The climate of Venice and its action on monument decay. Proc 4th Int Symp Conservation of monuments in the Mediterranean. 2:53–65

Camuffo D, Sturaro G, Valentino A (1999a) Urban climatology applied to the deterioration of the Pisa Leaning Tower, Italy. Theor Appl Climatol 63:223–231

Camuffo D, Sturaro G, Valentino A (1999b) Thermodynamic exchanges between the external boundary layer and the indoor microclimate at the Basilica of Santa Maria Maggiore, Rome, Italy: the problem of conservation of ancient works of art. Boundary Layer Meteorol 92:243–262

Caneva G, Gori EG, Danin A (1992) Contributo della pioggia battente alla colonizzazione biologica di superfici murarie di Roma. Boll Geofis 15(3):119–131

Cantù V (1977) The climate of Italy. In: Wallén CC (ed) Climates of central and southern europe. Elsevier, Amsterdam, p 127–183

Clifford J (1981) Properties of water in capillary and thin films. In: Franks F (ed) Water, a comprehensive treatise. Vol 5. Water in disperse systems. Plenum Press, New York, p 75–132

Colacino M, Dell'Osso L (1980) The local atmospheric circulation in the Rome area. In: Longhetto A (ed) Atmospheric

planetary boundary layer physics. Elsevier, Amsterdam, p 375–381
Colacino M, Purini R (1986) A study on the precipitation in Rome from 1782 to 1978. Theor Appl Climatol 37:90–96
Colacino M, Rovelli A (1983) The yearly averaged air temperature in Rome from 1782 to 1975. Tellus 35A:389–397
Del Monte M (1991) Trajan Column: lichens don't live here any more. Endevour 15(2):86–89
Del Monte M, Sabbioni C (1986) Chemical and biological weathering of an historical building: the Reggio Emilia Cathedral. Sci Tot Environ 50:147–163
Eredia F (1911) Il Clima di Roma. Esame delle osservazioni meteorologiche eseguite dal 1782 al 1910. Bertero, Rome
Everett DH (1961) The thermodynamics of frost damage to porous solids. Trans Faraday Soc 57:1541–1551
Fagerlund G (1973) Determinations of pore-size distribution from freezing point depression. Mater Construct 6: 215–225
Gauri KL, Bandyopadhyay JK (1999) Carbonate stone. Chemical behaviour, durability and conservation. Wiley-Interscience, New York
Ginell WS (1994) The nature of changes caused by physical factors. In: Krumbein WE, Brimblecombe P, Cosgrove DE, Stainforth S (eds) Durability and change. Wiley, New York, p 81–94
Iribarne JV, Godson WL (1986) Atmospheric thermodynamics. Reidel, Dordrecht
Koestler RJ, Brimblecombe P, Camuffo D, Ginell WS, Graedel TE, Leavengood P, Petushkova J, Steiger M, Urzì C, Vergès-Belmin V, Warscheid T (1994) How do external environmental factors accelerate change? In: Krumbein WE, Brimblecombe P, Cosgrove DE, Staniforth S (eds) Durability and change—the science, responsibility and cost of sustaining cultural heritage. Wiley, Chichester, p 149–163
Kraus EB, Businger JA (1994) Atmosphere-ocean interaction. Oxford University Press, New York, and Clarendon Press, Oxford
Laurenzi Tabasso M, Marabelli M (1992) Il degrado dei monumenti in Roma in rapporto all'inquinamento atmosferico. Betagamma, Viterbo
Lorusso S, Marabelli M, Viviano G (1995) La contaminazione ambientale e il degrado dei materiali di interesse storico-artistico. Bulzoni, Rome
Lunardini VJ (1991) Heat transfer with freezing and thawing. Elsevier, Amsterdam
Mangianti F, Beltrano MC (1995) Le precipitazioni a Roma. UCEA, Rome
Mason BJ (1971) The physics of clouds. Clarendon Press, Oxford
Mennella C (1967) Il clima d'Italia. Conte, Neaples
Meteorological Office (1962) Weather in the Mediterranean, Vol 1. Meteorological Office 391, London
Pombo Fernandez S, Nicholson K, Urquhart D (1999) Removal and analysis of soluble salts from chemically cleaned sandstones. In: Jones MS, Wakefield RD (eds) Aspects of stone weathering, decay and conservation. Imperial College Press, London, p 77–89
Reiter E (1975) Handbook for forecasters in the Mediterranean. Environmental Prediction Research Facility, Monterey, CA
Weast RC (1985) CRC Handbook of chemistry and physics 1985–86, 66th edn. CRC Press, Boca Raton, FL, p D213–D214
Winkler EM (1994) Stone in architecture. Springer-Verlag, Berlin
Zezza F (ed) (1996) Origin, mechanisms and effects of salts on degradation of monuments in marine and continental environments. European Commission Research Report No. 4, Bari

Editorial responsibility: Mike Hulme, Norwich, United Kingdom

Submitted: September 16, 1999; Accepted: June 26, 2000
Proofs received from author(s): October 27, 2000